

# Investigation of the Compton effect

Máté Csanád

Eötvös University, Department of Atomic Physics

February 13, 2016



Supported by the Higher Education Restructuring Fund  
allocated to the Eötvös University by the Hungarian Government

## 1 Thomson scattering

The effect of electromagnetic radiation on atoms was intensively investigated in the beginning of the 20<sup>th</sup> century (c.f. atomic spectra, photovoltaic and photoelectric effect). In the classical picture, electromagnetic radiation is the spatial and temporal alternation of electric and magnetic field. These fields affect the charges inside atoms, and accelerate them. The accelerating charges then radiate: this is the so-called Thomson scattering. [1]

Classically, the frequency of the incoming and outgoing waves is identical (c.f. excited oscillation). If the intensity is large enough, the atom may be repelled by it, and the Doppler effect may change the frequency of the observed outgoing wave [2], this is however negligible at small intensities. See the left plot of Fig. 1 for an illustration of the Thomson-scattering. Note that in this case, the spatial distribution of the outgoing waves is symmetric to 90 degrees, i.e. the forward and backward directions are identical - the oscillating charge “does not know” the direction of the incoming wave, only the direction

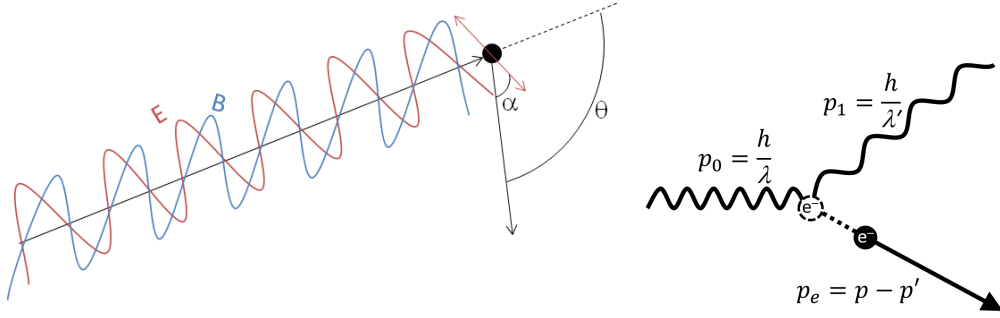


Figure 1: Scattering of electromagnetic waves, classically (Thomson scattering, left) and in quantum mechanics (Compton scattering, right).

of the oscillating electric field. The differential cross-section in this case is (expressed with the deflection angle  $\theta$ ):

$$\frac{d\sigma}{d\Omega} = r_0^2(1 + \cos^2 \theta) \quad (1)$$

where  $r_0 = \frac{ke^2}{m_e c^2} = 2,82 \cdot 10^{-15}$  m is the classical electron radius.

As we will see in the next section, for high frequency electromagnetic radiation, both of the above two statements (unchanged frequency, symmetrical distribution) are falsified by the experiment.

## 2 The Compton effect

In 1922 Compton observed the scattering of X-ray radiation on paraffin [3]. He detected large wavelength components in the scattered waves (even at low incoming intensity), in contradiction to the classical theory. The distribution of the scattered waves was not symmetric to 90 degrees, also contradicting the classical theory. These facts can only be explained in terms of quantum mechanics, postulating electromagnetic radiation to be quantized, i.e. the existence of photons. The scattering is then the elastic collision of photons and electrons (almost unbound, compared to the photon energy).

Photons carry an energy of  $E = h\nu = hc/\lambda$ , where  $\nu$  is the frequency of the radiation,  $\lambda$  its wavelength, while  $h$  is Planck's constant and  $c$  the speed of light. They also have a momentum of  $|\mathbf{p}| = E/c = h/\lambda$  (c.f. de Broglie wavelength). Let us note the relationship between the four-velocity associated to a photon, its  $\gamma$  factor and the three dimensional

velocity:

$$u^\mu = \gamma(c, \mathbf{v}) \quad (2)$$

$$u^\mu u_\mu = \gamma^2(c^2 - \mathbf{v}^2) = c^2 \quad (3)$$

$$\gamma = \frac{1}{\sqrt{1 - \beta^2}}, \quad \beta = \frac{|\mathbf{v}|}{c} \quad (4)$$

The relationships between energy, mass, four-momentum and three-momentum are:

$$E = mc^2\gamma \quad (5)$$

$$\mathbf{p} = m\mathbf{v}\gamma \quad (6)$$

$$p^\mu = (E/c, \mathbf{p}) = mu^\mu \quad (7)$$

$$p^\mu p_\mu = m^2 u^\mu u_\mu = m^2 c^2 \quad (8)$$

$$E^2 = m^2 c^4 + |\mathbf{p}|^2 c^2. \quad (9)$$

Conservation of energy and momentum holds for the Compton scattering (see fig. 1):

$$\mathbf{p}_0 = \mathbf{p}_e + \mathbf{p}_1, \quad (10)$$

$$m_e c^2 + E_0 = E_e + E_1, \quad (11)$$

where the electron in the beginning has only the energy corresponding to its rest mass. From eq. (11), as for photons  $E = |\mathbf{p}|c$  holds, we get

$$m_e c^2 + \mathbf{p}_0 c = \sqrt{\mathbf{p}_e^2 c^2 + m_e^2 c^4} + \mathbf{p}_1 c \quad (12)$$

where  $\mathbf{p}_1$  and  $\mathbf{p}_0$  are the momenta of the photon before and after the collision, while  $\mathbf{p}_e$  is the electron momentum after the collision, and  $m_e$  is the electron rest mass. From now on,  $p = |\mathbf{p}|$  for any momenta. Then, from the conservation of momentum:

$$\mathbf{p}_e = \mathbf{p}_0 - \mathbf{p}_1, \text{ i.e.} \quad (13)$$

$$p_e^2 = p_0^2 + p_1^2 - 2p_0 p_1 \cos \theta. \quad (14)$$

Here  $\theta$  is the scattering angle of the photon. From eq. (12) we get

$$p_e^2 = p_0^2 + p_1^2 + 2p_0 m_e c - 2p_0 p_1 - 2p_1 m_e c. \quad (15)$$

This can be plugged in the previous equation, and we get for the momentum of the scattered photon:

$$p_1 = \frac{p_0}{1 + \frac{p_0}{m_e c}(1 - \cos \theta)} \quad (16)$$

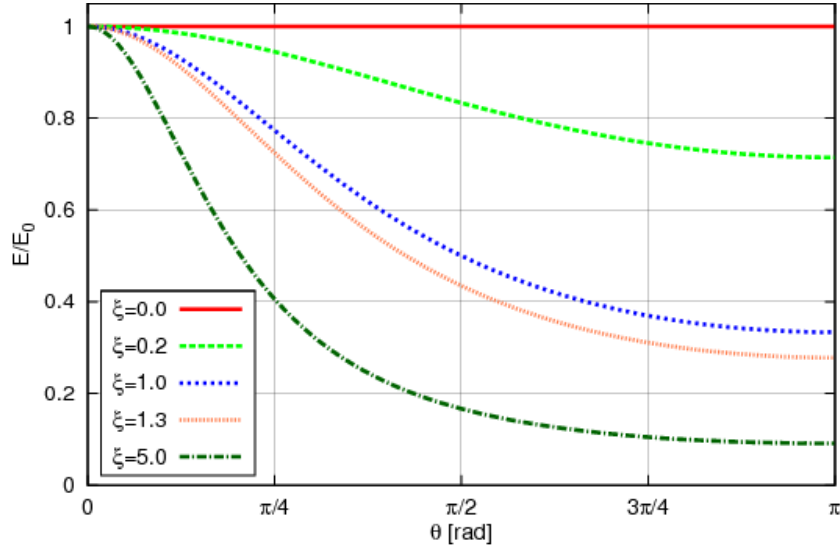


Figure 2: Energy of the scattered photon versus its scattering angle. For large values of relative photon energy  $\xi = E_0/m_e c^2$ , scattered photons lose much of their energy.

which can be translated to the energy change of the photon:

$$\frac{E_1}{E_0} = \frac{h\nu_1}{h\nu_0} = \frac{1}{1 + \xi(1 - \cos\theta)} = P, \quad (17)$$

where  $\xi = \frac{p_0}{m_e c} = \frac{h\nu_0}{m_e c^2}$ , and we introduced  $P$  as the energy of the scattered versus of the original photon.  $P$  then depends on  $\theta$  and  $\nu_0$ , the original frequency. Thus, according to Compton's observations, the energy of the scattered photon decreases with increasing scattering angle, and its wavelength increases. As shown in fig. 2, for small incident energies ( $\xi \ll 1$ )  $E_1 \approx E_0$ , while for very energetic photons ( $\xi \gg 1$ ),

$$E_1 = \frac{m_e c^2}{1 - \cos\theta}. \quad (18)$$

### 3 Angular distribution of Compton scattering

Angular distribution of Compton scattered photons was derived in 1928 by Oskar Klein and Yoshio Nishina, and was one of the first results obtained from the study of quantum electrodynamics. [4]. According to this formula, the cross-section of the scattering of a photon in a solid angle region  $d\Omega$  around an angle  $\theta$  is [5]

$$\frac{d\sigma}{d\Omega} = r_0^2 \frac{1 + \cos^2\theta}{2} \frac{1}{(1 + \xi(1 - \cos\theta))^2} \left[ 1 + \frac{\xi^2(1 - \cos\theta)^2}{(1 + \cos^2\theta)(1 + \xi(1 - \cos\theta))} \right] \quad (19)$$

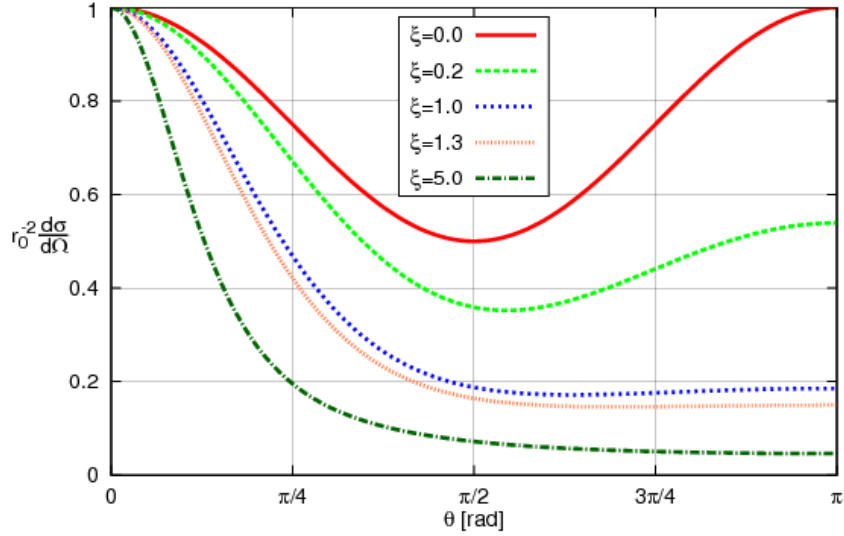


Figure 3: Angle dependence of the cross-section of Compton-scattering. For  $\xi = 0$ , the Thomson scattering curve is recovered.

where  $r_0 = \frac{ke^2}{m_e c^2} = 2,82 \cdot 10^{-15}$  m, the classical electron radius, and  $d\Omega = 2\pi \sin \theta d\theta$  (as the process is invariant to rotations around the axis of the incoming particle). If we use the previously defined ratio  $P = (1 + \xi(1 - \cos \theta))^{-1}$  then our formula becomes:

$$\frac{d\sigma}{d\Omega} = \frac{r_0^2}{2} (P - P^2 \sin^2 \theta + P^3). \quad (20)$$

In Fig. 3. we plotted the quantity  $\frac{1}{r_0^2} \frac{d\sigma}{d\Omega}$  versus scattering angle for a few  $\xi$  values. As Eq. (20) shows, in case of  $\xi \rightarrow 0$  (or equivalently  $P \rightarrow 1$ ) the cross-section is proportional to the  $(2 - \sin^2 \theta) = (1 + \cos^2 \theta)$  term, i.e. we get back the classical Thomson-formula. For small  $\xi$  values, the difference between forward and backward scattering is not large, but for large  $\xi$  values, the probability of forward scattering ( $\theta > \pi$ ) is much smaller. Even for  $\xi \approx 0.2$  (hard X-ray radiation) the curve differs strongly from the Thomson-formula, denoted by the solid red curve in Fig. 3.

## 4 Measurement details

In our laboratory exercise we use a  $^{137}\text{Cs}$  source, which had an activity of 486.55 MBq on July 1, 1963. The half-life of this isotope is 30.17 years, and it decays by negative beta decay to an excited  $^{137}\text{Ba}$  nucleus. This in turn decays with 94.4% probability and 2.55 minutes half-life to a stable  $^{137}\text{Ba}$  nucleus, and emits a 662 keV photon in the process. See the decay scheme in Fig. 4. We will analyze the Compton scattering of these 662

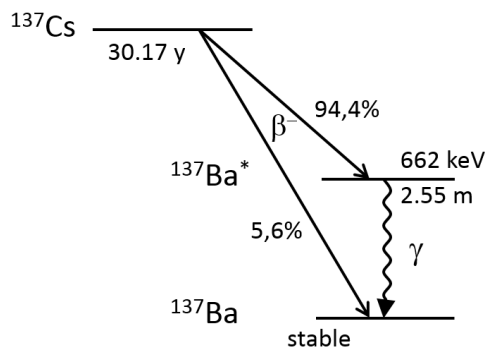


Figure 4: Decay scheme of  $^{137}\text{Cs}$ .

keV photons in our analysis. The current activity of the source can be calculate from the  $A(t) = A(0) \cdot 2^{-t/T}$  relationship, with  $T$  being the half life.<sup>1</sup>

Our source emits a considerable amount of energy in form of  $\gamma$  radiation, which may be harmful from a short distance. So we should never touch the source with bare hands, but rather with a tweezer. Also, during the lab exercise, lead shielding shall always protect us from the radiation. This way we adhere to the ALARA principle by keeping the absorbed dose to a reasonable minimum.

Our goal in this exercise is to measure the scattered photon energy as a function of the scattering angle and compare measurement results to the formula of Eq. (17). We will also investigate the differential cross-section versus the scattering angle and compare it to Eq. (3), the Klein-Nishina formula. As our measurement setup includes a coincidence circuit (in the analog-digital converter), we also test the coincidence of the ejected electron and the detected photon, with a timing accuracy of  $10^{-6}$  s. The measurement setup is shown in Fig. 5.

The 662 keV gamma-photons (from the  $^{137}\text{Ba}$  isotope) are directed on the target by a lead collimator. This simply shields all radiation that would not go into the desired direction: from the  $4\pi$  solid angle, it only lets photons from the source (being on one end of the collimator) go through if they are going into the direction of the small opening on the other end of the collimator.

The scattering occurs on a plastic scintillator, thus the target is also used to detect the ejected electrons. The signal from this electron detector is amplified and converted to a shape that can be later used as a gate signal by our coincidence circuit inside the analog-digital converter. The gamma detector (NaI(Tl) scintillator) is placed at an angle of  $\theta$ , and its signal is digitized by the analog-digital converter (in fact a multichannel analyzer).

<sup>1</sup>This relationship can be inferred from  $N(t) = N(0) \cdot e^{-\lambda t} = N(0) \cdot 2^{-t/T}$ , which is the exponential decay law.

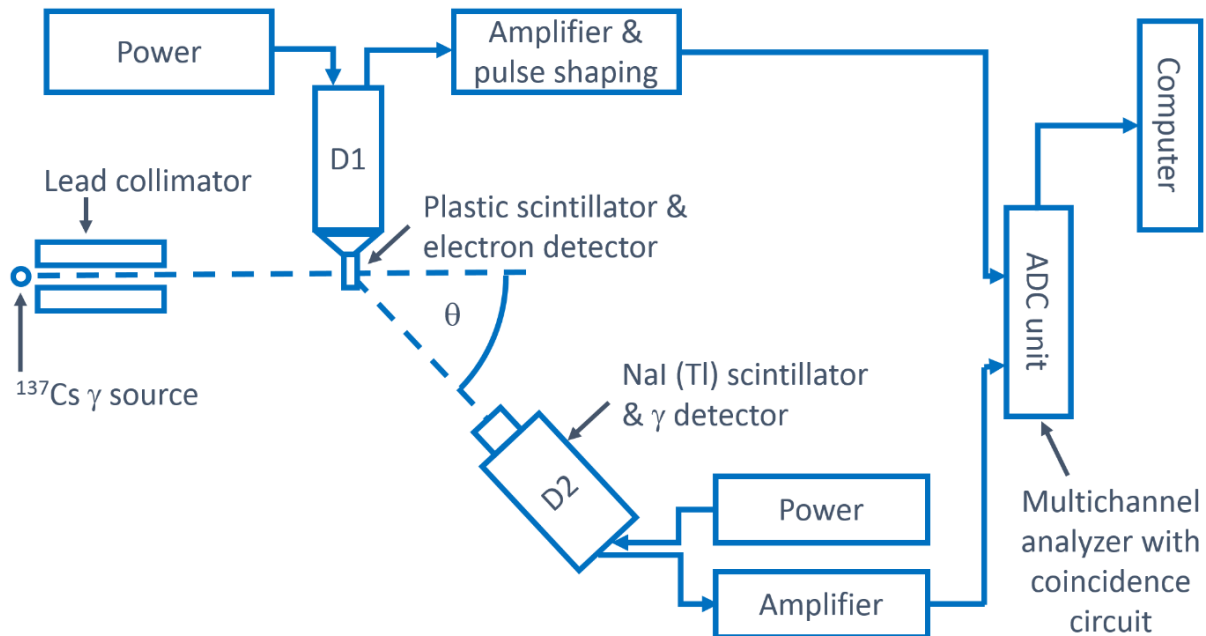


Figure 5: Logical setup of our measurement.

It is enough to sample the gamma spectra with 128 channels, in a couple different  $\theta$  settings. The location of the Compton peak will tell us the energy of the scattered photons, while the area under the peak (and the measurement duration) will tell us the intensity of the scattered radiation, thus the differential cross-section. In order to do so, we will need to know the efficiency of our NaI(Tl) detector. This was measured beforehand, and is plotted on Fig. 6. The following empirical formula describes the photon energy ( $E$ ) dependence of the efficiency (averaged on the total detector area):

$$\eta = 0,98e^{-E/(0,21MeV)} + E/(20MeV) \quad (21)$$

This result is largely influenced by the decrease of the photo-effect cross-section with increasing energy. During the measurement, we will need this averaged efficiency to calculate the true number of incoming photons. However, if we would like to calculate the number of incoming photons at  $0^\circ$ , i.e. the incoming photon flux, we will need the location-dependent efficiency: the area hit by the photons may be smaller than the total detector area. The efficiency as a function of distance from the detector center can be given by this empirical formula:

$$\eta = \frac{0,123}{1 + e^{(|r|-17,6mm)/3,6mm}} \quad (22)$$

(see Fig. 6).

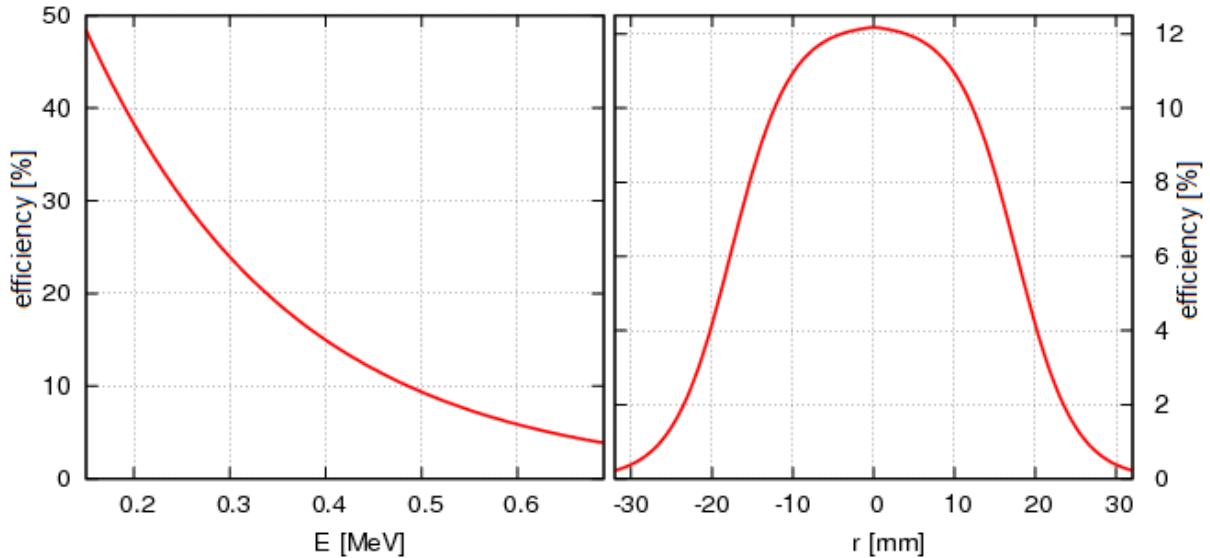


Figure 6: The photo-peak efficiency of the NaI(Tl) detector, averaged on the total detector area, as a function of incoming photon energy (left plot); efficiency at 662 keV as a function of distance from the symmetry axis (center) of the detector (right plot).

## 5 Measuring the energy of the scattered photon

The incoming high-energy photons generate light in the scintillator material. The light creates photoelectrons through the photo-effect, which is then converted to an electronic signal by a photoelectron-multiplier. This signal is digitized by the AD converter, and appears as a hit in one of the channels of the multichannel analyzer (if coincidence mode is used, then the hit is registered only in case of a coincident gate signal from the electron detector). Our measurement results then in a histogram of hits, with the channel number being on the horizontal axes. For an example, see Fig. 7.

In coincidence-enabled measurements, a Compton peak appears at a location depending on the detector angle  $\theta$ , corresponding to the energy of the photons scattered in the given direction. Left from the peak we see the Compton spectrum with the Compton edge. The spectrum corresponds to the photons that scatter off the scintillator but escape from the detector. These deposit only a fraction of their energy in the scintillator material, thus creating a variable sized signal. The maximum of energy deposition happens in case of fully back-scattered photons, and their registered signal size corresponds to the Compton edge.

The channel number then has to be converted to energy, by calibrating our device. The known 662 keV energy of not scattered photons (that hit the detector placed at  $\theta = 0^\circ$  by going through the electron target without scattering) is a known point we can

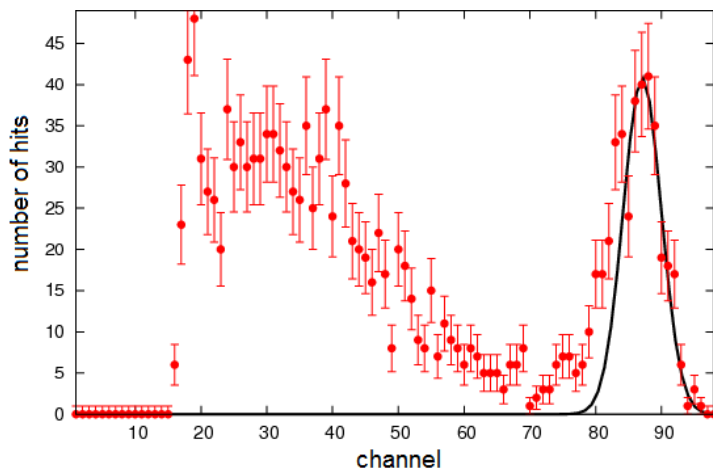


Figure 7: A spectrum from the multichannel analyzer, from pulses in coincidence with the electron detector. The measurement was performed with the photon detector at  $\theta = 30^\circ$ . The Compton scattered photons appear near channel 90, and below that we see the Compton edge and the Compton spectrum. The first channels pick up a large amount of electronic noise, so we exclude them from our measurement. We then fit a Gaussian on the Compton peak, to determine its location and area exactly. The far left side of the peak can be left out of the fit, since this part contains hits from the Compton edge as well.

use to calibrate. However, the energy-channel number connection can be affine linear as well, i.e. we are looking for an  $E = a \cdot x + b$  correspondence (with  $x$  being the channel number and  $a, b$  the calibration constants). In order to find  $a$  and  $b$ , we need another point. This could be the  $K_\alpha$  line of lead, as the energy of this is known to be 75 keV (c.f. Moseley's law). During  $K_\alpha$  transition, an outer electron from the 2p shell transitions to the 1s shell (from where another electron was ejected by a photon), and the transition energy is radiated out in form of a photon. This photon can be detected, if coincidence is turned off. Without coincidence, we see other peaks beyond the  $K_\alpha$  line and the Compton peak as well, e.g. the peak of back-scattered photons that come from behind our photon detector. However, the  $K_\alpha$  line can be identified by having a lower energy than any of these. This can be verified by plugging  $\theta = \pi$  into Eq. (17).

The calibration using the above mentioned two points goes as follows. First, we fit a Gaussian on the peaks, and determine their locations  $x_1$  and  $x_2$ . Then, knowing the corresponding energies  $E_1$  and  $E_2$ , we solve the equations

$$E_1 = a \cdot x_1 + b, \quad E_2 = a \cdot x_2 + b \quad (23)$$

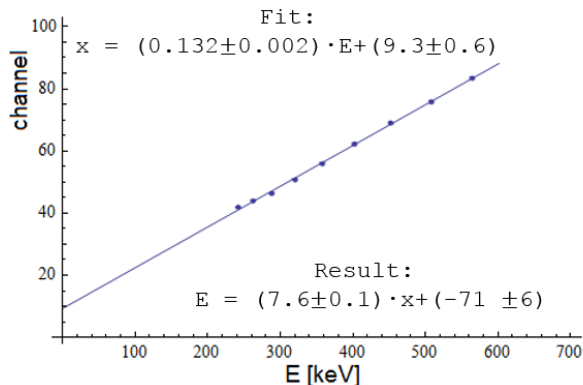


Figure 8: An example calibration based on actual data measured at 9 different angles

and get

$$a = \frac{E_1 - E_2}{x_1 - x_2}, \quad b = \frac{E_2 x_1 - E_1 x_2}{x_1 - x_2}. \quad (24)$$

As both  $x_1$  and  $x_2$  are given with some uncertainty (from the Gaussian fits), these propagate to create an uncertainty of  $a$  and  $b$  (via standard error propagation). Then, in all subsequent measurements  $E = a \cdot x + b$  can be used, and the uncertainty of  $E$  be determined. Note however, that the parameter uncertainties  $\Delta a$  and  $\Delta b$  are systematic errors, so in case of a  $\chi^2$  test, they should not be taken into account (only the “statistical”, point-by-point independent uncertainty of  $x$ ,  $\delta x$ ).

This type of calibration suffers however from a deficiency. We measured both previously mentioned peaks without using the coincidence circuit, at a high hit rate, whereas all subsequent measurement will be performed with coincidence, at a very low hit rate. It may happen, as it does in our case, that the multichannel analyzer has a difference “pulse height to energy” conversion in the two settings. So we will perform a different type of calibration. We measure the location of the Compton peak (expressed in channel number), and plot this versus the theoretically calculated photon energy at the given angle  $\theta$ . Then we can fit a linear on this plot, by inverting this linear, we obtain the calibration equation  $E = a \cdot x + b$  (and calculate parameter uncertainties by standard error propagation). See an example calibration result in Fig. 8.

## 6 Cross section measurement

The cross-section  $\sigma$  of a scattering process can experimentally defined as:

$$\frac{\Delta N_{\text{scattered}}}{\Delta t} = N_{\text{target}} j \sigma \quad (25)$$

where  $\Delta N_{\text{scattered}}$  is the number of scattered particles in a  $\Delta t$  time interval, while  $N_{\text{target}}$  is the number of scattering centers in the target (electrons, in our case). Furthermore,  $j$  is the incoming photon flux, and  $\sigma$  is called the total cross section of the given process. We can also define the differential cross section, utilizing  $A$ , the common area of the photon beam and the target,  $dx$ , the thickness of the target, and  $n$ , the number density of scattering centers in the target. The result is:

$$\frac{\Delta N_{\text{scattered}}}{\Delta t} = jAdxn\Delta\Omega \frac{d\sigma}{d\Omega} \quad (26)$$

where  $\Delta\Omega$  is the solid angle covered by our photon detector (as seen from the target). The product  $jA$  is then the number of photons coming from the source and hitting the target. As at this energy, all electrons can be approximated with being free electrons, the number of target particles can be calculated as the electron number density in the target:

$$n = \frac{\rho N_A Z}{M}, \quad (27)$$

with  $\rho$  being the density of the target (1.03 g/cm<sup>3</sup> in our case),  $Z$  the number of electrons within a molecule of the target,  $M$  is the molar mass of the target molecules, while  $N_A$  is the Avogadro number. As our target is a plastic scintillator, it can be viewed as being built up by CH<sub>2</sub> blocks, thus  $Z = 8$  and  $M = 14$  g/mol are reasonable assumptions.

It is also important to consider the efficiency of our detector. If we detect  $\Delta N$  particles, then with an efficiency if  $\eta$ , the original number of particles hitting the detector can be given as  $\Delta N/\eta$ . Based on all this, the differential cross section can be calculated as:

$$\frac{d\sigma}{d\Omega} = \frac{\Delta N_{\text{scattered}} M}{jAdx\rho N_A Z \Delta\Omega \eta \Delta t} = \frac{K}{\eta} \cdot \frac{\Delta N_{\text{scattered}}}{\Delta t} \quad (28)$$

where  $K = M/(jAdx\rho N_A Z \Delta\Omega)$ , and its value is the same for all angles, so it can be calculated just based on our experimental setup. Finally, by measuring the number of photons scattered to our detector, we measure the differential cross-section, and can check the Klein-Nishina formula. From Eq. (20), we get

$$\frac{1}{K} \frac{d\sigma}{d\Omega} = \frac{1}{\eta} \cdot \frac{\Delta N_{\text{scattered}}}{\Delta t} = \frac{r_0^2}{2K} (P - P^2 \sin^2 \theta + P^3), \quad (29)$$

where the left side is measured (and the cross-section is already given), while the right side contains theoretical results. These two can be then directly compared, via the methods described in the next section.

## 7 Interpretation of the results

In the above sections, two measurements were discussed, and the theoretical calculations that can be directly compared to them. How do we interpret these comparisons, i.e. how do we interpret our results so far? In order to do so, we have to take into account the uncertainties of the results. The statistical error of our measurements comes from counting a finite number of hits. These numbers are distributed by a Poisson distribution, and thus the statistical uncertainty of a given count (number) can be approximated by the square root of the number itself, i.e.

$$\Delta N = \sqrt{N} \quad (30)$$

Thus if we get 100 hits in a given channel, the uncertainty of that is 10%. This uncertainty is point-by-point independent, i.e. there is no correlation between the size and sign of the uncertainty of the channel hit numbers. Based on this information, we can estimate the “probability” of the theoretical calculation, given the experimental results. First, we define the distance of the two:

$$\chi^2 = \sum_{i=1}^N \frac{(f(x_i) - y_i)^2}{\Delta y_i^2} \quad (31)$$

where  $x_i$  are the locations of the measurement points (the angle  $\theta$  in our case),  $y_i$  are the measurement result (the measured photon energy or cross-section), while  $\Delta y_i$  represent the uncertainty of each measurement. Furthermore,  $f(x_i)$  is the to-be-tested theoretical result, as a function of measurement setting  $x_i$ . In case of an exactly true theory and a perfect measurement,  $f(x_i) = y_i$ , but usually, the two differ, ideally “within errors”, i.e. the  $\chi^2$  contribution of each  $i$  is near to or below 1. Note, that for a high number of measurements, most probably there will be points with large  $\chi^2$  contributions, but the overall  $\chi^2$  value shall remain close to or below the number of measurements.

The obtained  $\chi^2$  can then be evaluated with the so-called  $\chi^2$  test, which gives us the probability that, given the theory was true, with what probability would our measurement differ from the theory by a value equal to or greater than the obtained  $\chi^2$ . This can also be interpreted as the probability of the theory being true. If the number of measurement points (angle settings in our case) is  $N$ , then the  $\chi^2$  probability density can be calculated as (assuming the uncertainties are independent):

$$\tilde{P}(\chi^2, N) = \frac{1}{2^{N/2} \Gamma(N/2)} (\chi^2)^{N/2-1} e^{-\chi^2/2} \quad (32)$$

where if  $N/2 \in \mathbb{Z}$ ,  $\Gamma(N/2) = (N/2 - 1)!$ , otherwise the general  $\Gamma$  function has to be used. The expectation value of  $\chi^2$  is  $N$ , so sometimes the relative value of  $\chi_r^2 = \chi^2/N$  is also given.

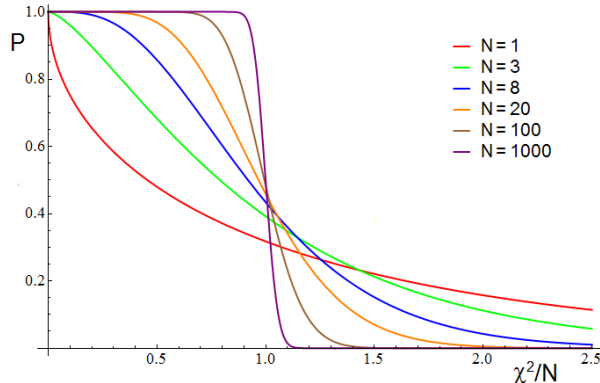


Figure 9: The probability  $P(\chi_M^2, N)$  as a function of the measured  $\chi_M^2$ , for various  $N$  values. For high  $N$  values, the probability sharply drops near  $\chi_M^2/N = 1$ . This means, that for large  $N$ , the probability of  $\chi^2 > N$  goes to zero.

The goodness of the fit is then given through the integral of the above function, from zero to  $\chi_M^2$ , the actually measured  $\chi^2$  value. This integral represents the probability of measuring a theory-data difference less than  $\chi_M^2$ . So the expression

$$P(\chi_M^2, N) = 1 - \int_0^{\chi_M^2} \tilde{P}(\chi^2, N) d\chi^2 = \frac{1}{\Gamma(N/2)} \gamma(N/2, \chi^2/2) \quad (33)$$

gives us the probability of measuring a difference that is at least  $\chi_M^2$  (where  $\gamma$  is the incomplete gamma function). This is sometimes called the confidence level of the data-theory comparison. Note furthermore, that if the theoretical results has parameters that are fitted to the data, the number of free parameters should be subtracted from  $N$ , which then means the number of degrees of freedom:  $N = N_{datapoints} - N_{parameters}$ . For an illustration of how  $P(\chi_M^2, N)$  depends on  $\chi_M^2$ , see Fig. 9.

It is important to keep in mind that the measurement may contain systematic or correlated errors, which are correlated from point to point. These errors include for example the uncertainty of the detector efficiency: if this is underestimated, then all data points should move up. In our measurement, the main source of systematic errors is the calibration, through which we calculate the energy from the channel number. Systematic error  $\delta y_i$  can be taken into account by modifying  $\chi^2$  to

$$\chi^2 = \sum_i \frac{(f(x_i) - y_i + \alpha \delta y_i)^2}{\Delta y_i^2} \quad (34)$$

where  $\alpha$  is a number between  $-1$  and  $+1$ . This essentially means that we move all data points up or down by a  $< 1$  multiple of their correlated uncertainty. Then we can search

for a minimum by varying  $\alpha$ ; however, it is important to see that  $\alpha \neq 0$  diminishes the probability of the final measurement. This is usually taken into account by adding a  $\chi_{\text{sys}}^2$  term to the  $\chi^2$  and calculating the confidence level (probability) with this additional term.

It may seem strange to discuss uncertainties and measurement errors for so long, but this is a very important point in physics. A measurement can only falsify a theory, if their difference makes it extremely unlikely to both being true. But this likelihood has to be evaluated carefully. For a single point to lie at least one unit of uncertainty ( $1\sigma$ ) away from the theoretical value the probability is 32%. For two units of uncertainty ( $2\sigma$ ), the probability is around 5%. This means essentially, that for 1 in 20 measurements, we will have one point being two uncertainties away from the theoretical curve, even if both the theory and the measurement are right. A  $3\sigma$  difference has however only 0.3% probability, so that is usually regarded as the “discovery limit”. In particle physics, having an immense amount of data at hand, usually  $5\sigma$  is required to announce “discovery”.<sup>2</sup>

## 8 Measurement tasks

During the laboratory exercise, we measure the gamma spectrum with the photon detector at several different  $\theta$  angle settings. Then a laboratory report shall be prepared, which should detail all the below mentioned tasks. One should go into detail how each task was done, with reference to present note where needed (without repetition of too long parts of this note).

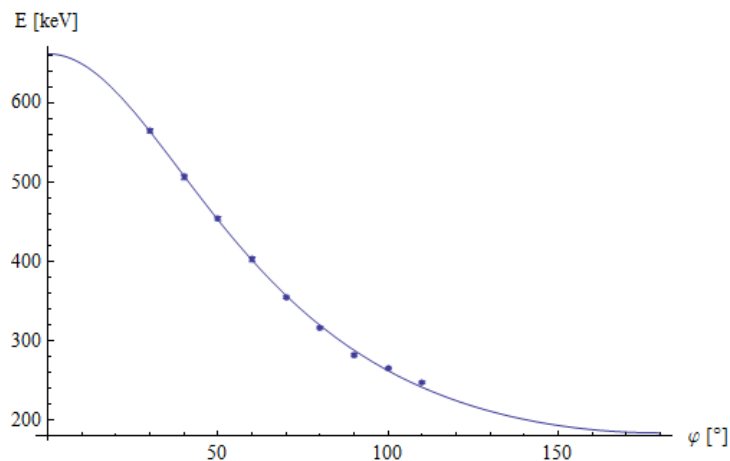
1. Estimate the activity of the source based on the given activity in 1963 and half-life  $T$ . Calculate the power of the source, assuming the 662 keV energy of the radiated photons. Give an upper limit on the absorbed dose ( $[\text{Gy}] = [\text{J/kg}]$ ), by dividing the absorbed energy by the mass of the absorbing tissue. As we are dealing with gamma radiation, this equals the effective dose, measured in units of Sievert ( $[\text{Sv}] = [\text{J/kg}]$ ). Compare this to the 2.4 mSv average annual effective dose that an average person absorbs. Based on all above, calculate the ratio of the maximal absorbed effective dose to the average daily dose. First, assume that all of the radiation was absorbed (which would only be possible if we would have swallowed the source). Then, assume being 1 meter away from the source (and having a body area of  $0.5 \text{ m}^2$ ). In reality, the lead shielding reduces this dose by multiple orders of magnitude. Estimate this, too, by assuming that a fraction of  $1/e$  of the photons pass through a 6 mm thick lead wall, and our shielding is 6 cm thick.
2. Measure all of the geometric parameters of the measurement setup (collimator, target and detector areas and distances), and show these on a schematic drawing.

---

<sup>2</sup>All of these probabilities assume normally distributed variables.

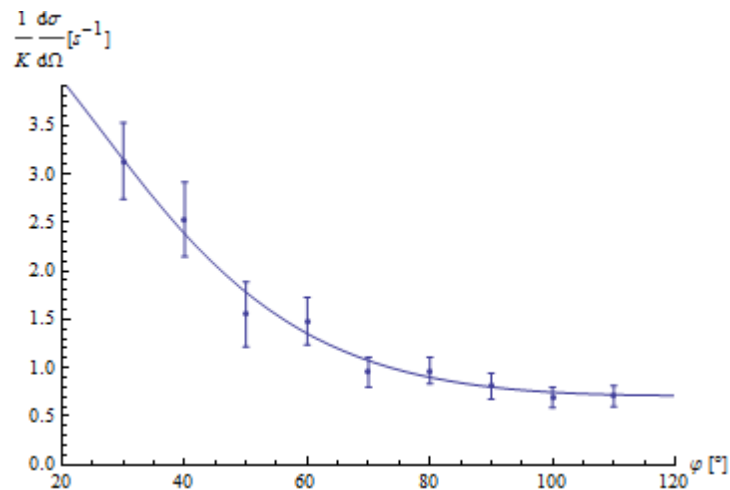
Calculate the size of the photon beam at the target and at the gamma detector. Compare this to the sizes of the mentioned units. Based on this, calculate the number of photons hitting the gamma detector at  $\theta = 0$  – if the whole photon beam hits the detector, then this number equals the number of photons coming out of the collimator. Measure this also directly, and compare the measurement and the calculation (using the known efficiency of the source). In the next tasks, use the measured version.

3. Calibrate the multichannel analyzer with the direct photon peak at  $\theta = 0$  and with the lead  $K_\alpha$  line of 75 keV measured at  $\theta \approx 0$  (so that photons have a chance to hit the lead detector container). Both measurements shall be done without coincidence.
4. Measure the photon spectrum (with coincidence from the electron detector) in at least 8-10  $\theta$  settings, such that we get at least 30-40 hits at the maximum of the Compton-peak (this should take around 15 minutes for each measurement). Fit a Gaussian on all peaks (maybe leaving out the points on the far left side of the peak), and determine the location of the maximum. Plot this maximum versus the calculated photon energy, and fit an affine linear on it. Compare this calibration to the previous one.
5. With the new calibration, plot the angle dependence of the energy of the scattered photons. Determine the  $\chi^2$  distance of the Compton formula and the acquired data points. Analyze this with a  $\chi^2$  test, including the statistical and the systematic errors. See an example plot on the angle dependence of the scattered photon's energy based on real data below:



6. Based on the Gaussian fit, determine the number of photons in the Compton peak (by integrating the Gaussian). Calculate the differential cross-section from this,

based on Section 6. Compare the measurements to the  $d\sigma/d\Omega$  values of the Klein–Nishina formula of Eq. (20). Do this by leaving the  $\frac{r_0^2}{2K}$  parameter free, i.e. fit the (29) formula to the points calculated through the  $\frac{\Delta N_{\text{scattered}}}{\eta \Delta t}$  formula. Analyze the obtained  $\chi^2$ . Compare the obtained  $\frac{r_0^2}{2K}$  parameter to its theoretical value. See an example plot of the left and right hand sides of Eq. (29), based on real data below:



7. Compare the previously obtained  $K$  (by taking  $r_0$  as granted) and the value calculated from the thickness, density etc of the detector and the  $jA$  photon number. If there is a major difference, try to find the most important factors contributing to it.

## 9 Control questions

1. What kind of materials/particles are interacting in the Compton effect?
2. Draw a simple diagram describing the Compton effect (indicating particle types and momenta).
3. What is the relationship between a photons energy and wavelength?
4. What is the relationship between a relativistic particle's energy, four-momentum and mass?
5. What is the relationship between three-velocity and four-momentum?
6. Can a component of the three- or the four-velocity be bigger than the speed of light  $c$ ? If yes, why?

7. What is the relationship between the Compton scattered photon's energy and its scattering angle? Draw a graph and give a formula also.
8. Why is the Compton effect hard to explain in terms of classical physics?
9. What general physical relationships or formulas are sufficient to explain the wavelength shift in the Compton effect?
10. What is the angular distribution of Compton scattering? Why is it interesting?
11. For what theory is the Compton effect a good "proof", and why?
12. Define the total cross-section. What is its meaning in plain words?
13. Define the differential cross-section.
14. What kind of source do we use in our laboratory exercise, and what particles does it emit?
15. What is the decay scheme of  $^{137}\text{Cs}$ ?
16. How does the activity of a source depend on time?
17. How big is the approximate average effective yearly dose from natural sources?
18. How do we defend ourselves from the radiation that we could absorb during this laboratory exercise?
19. Suppose we have a 10 cm long collimator with a 3 mm wide tube. Let us put a 100 MBq (point-like) source on one end. How many photons are coming out on the other end of the collimator?
20. What is a plastic scintillator, and how do we use it in our measurement?
21. What is a NaI scintillator, and how do we use it in our measurement?
22. What is an analog-digital converter, and how do we use it in our measurement?
23. Where and how do we use a coincidence circuit in our measurement?
24. What is the scattering target in our setup? What else do we use it for?
25. Why can all electrons be regarded as target particles in our measurement?
26. Why is it important to know the uncertainties of our measurement?
27. Suppose we count 400 hits in a given channel. What is the relative uncertainty of this measurement?

28. What are the main ideas of the  $\chi^2$  test?
29. What is the difference between statistical and systematic errors?
30. When does a measurement falsify a theory?

## References

- [1] Jackson J. D. (1962) “*Classical Electrodynamics*”, Section 14.8
- [2] Moore, C. I. *et al.* (1995) “*Observation of the transition from Thomson to Compton scattering in multiphoton interactions with low-energy electrons*” *Phys. Rev. Lett.* **74** (13), 2439-2442
- [3] Compton, A. H. (1923) “*A Quantum Theory of the Scattering of X-Rays by Light Elements*” *Phys. Rev.* **21** (5): 483-502.
- [4] Klein, O.; Nishina, Y., (1929) “*Über die Streuung von Strahlung durch freie Elektronen nach der neuen relativistischen Quantendynamik von Dirac*”. *Z. Phys.* **52** (11-12): 853-869.
- [5] Weinberg, S. (1995). “*The Quantum Theory of Fields I*. pp. 362-9.